GeoJournal 24.1 103–117

A New Sensor System for Airborne Measurements of Maritime Pollution and of Hydrographic Parameters

Grüner, K., Dr., German Aerospace Research Establishment (DLR), Institute for Radio Frequency Technology, 8031 Weßling, Germany; Reuter, R., Dr., University of Oldenburg, Physics Department, 2900 Oldenburg, Germany; Smid, H., Bundesministerium für Verkehr, Robert-Schumannn-Platz, 5300 Bonn 2, Germany

ABSTRACT: Since 1986, two Dornier Do 28 D2 aircraft equipped with remote sensing instruments have been flown in the German responsibility areas of the North Sea and the Baltic Sea, aiming at a continuous surveillance of maritime pollution, and at an improved guidance of oil combating operations. Starting in 1991, a new DO 228-212 aircraft will be operated with improved performance. The sensor package will be completed with a new microwave radiometer and a laser fluorosensor, which allow measuring the volume of films on the sea surface, and classifying the substance type. Moreover, parameters which are relevant for the evaluation of ecological conditions as, for example, the occurrence of plankton blooms, can be obtained. The instruments work under control of a new central operator console which performs an in-flight evaluation of the sensor data, and transmission to ships and ground stations via data down link.

Introduction

Pollution of the sea has increased up to levels which can result in severe risks for the marine ecosystem. High loads of oil have been observed in many coastal waters. In the North Sea, the quantity of oil discharged at sea and being present in the form of spills on the sea surface is roughly estimated to about 30.000 to 90.000 tons per year (Tour d'Horizon surveillance flight programme, Schriel [1989]). Besides ship acoidents, a major source of these spills is assumed to be from the controlled release of oil by ship traffic and by oil production platforms.

In addition to the procurement of oil combating ships and other equipment, this situation has led to demands for airborne surveying methods. Basically, airborne surveillance shall meet two requirements: to provide helpful data for oil spill clean-up operations following accidental discharges, and to pursue the legal aspects of permanent contributions to marine oil pollution.

Aircraft equipped with remote sensing instruments have been provided in various countries in the period of 1983 to 1988 for a regular survey of coastal waters, see, for example, Lodge (1989). On the base of the sensor technology available at that time, their application shall render the following information:

- to detect spills over long distances, and to register their position and dimension
- to measure the thickness distribution of oil spills, and, hence, the pollutant quantity (violations of the MARPOL 1978 convention, Tab 1)
- to identify polluters with use of remotely sensed data and images that allow for a positive evidence
- to support and coordinate cleaning operations following accidental discharges of large quantities of pollutants, by navigational positioning of oil combating ships with respect to the central portions of spills.

Gathering these data must be feasible during day and night. Bad weather conditions like rain and fog should be as few a limiting factor as possible. Moreover, data shall be available during flight operations and in the form of imagery which allows easy and unambiguous interpretation by the operator.

The First Generation Maritime Surveillance System

Aircraft and Instrumentation

In 1986, two Dornier DO 28 D2 aircraft were procured by the Bundesministerium für Verkehr and by the federal coastal states of Bremen, Hamburg, Niedersachsen and Schleswig-Holstein for maritime surveillance in the

The marine pollution convention MARPOL 73/78 consists of 20 articles, which regulate the rights and obligations of parties, and of five annexes containing detailed regulations for the prevention of pollution by:

- ✧ mineral oils (Annex I)
- ✧ liquid chemicals carrid in bulk (Annex II)
- ✧ harmful substances carried in packaged forms (Annex III)
- ✧ sewage (Annes IV)
- ✧ garbage (Annex V).

Annexes I and II came into force in 1983 and 1987, respectively, with 44 states being parties at present. Annexes III to V have not yet been ratified (Bergmeijer, 1987).

The regulations of **Annex I on mineral oil discharges** are briefly summarized as follows:
Discharge conditions for oil tankers outside special areas are

- ✧ no discharge within 50 nautical miles from land, and
- ✧ maximum discharge of 60 litres per nautical mile outside this zone for tankers proceeding en route.

Bilge water discharges from ships require the use of oil/water separation equipment ensuring that

- ✧ the oil content does not exceed 15 ppm (parts per million) outside 3 nautical miles from the nearest coast, and
- ✧ 100 ppm outside 12 nautical miles from the nearest coast.

Discharges of oil are generally prohibited within special areas like, for example, the Baltic Sea.

Tab 1 The MARPOL 73/78 Convention

Federal Republic of Germany, and put into service in the beginning of 1988. Both aircraft are operated by the Naval Air Wing 5 in Kiel-Holtenau.

To meet the requirements for an efficient operation, the aircraft have to be ready for take-off within two hours following an alert. An endurance of 5 hours has to be achieved, with 2 to 3 hours of operation over the area of interest at a flight altitude of 1000 to 2000 ft. The flight range can reach 700 nautical miles.

The following instruments from Swedish Space Corporation (SSC) were integrated by Dornier, Friedrichshaven, into the surveillance aircraft:

- a Side-looking Airborne Radar (SLAR) for detecting slicks over long distances,
- a UV/IR Line Scanner for mapping the distribution of oil film thickness,
- an operator console for displaying TV images, SLAR and UV/IR scanner data on two TV monitors.

TV and hand-held cameras for documentation complete the sensor package. In 1987, a microwave radiometer was additionally integrated into one aircraft for mapping of the thickness distribution of accidental spills with large discharged volumes. Selected specifications of these sensors are given in Tab 2.

Measuring Principles of the Sensors

The Side-looking Airborne Radar

The SLAR is a long-ranging active sensor which allows for identifying slicks on the sea surface. Pulses in the 10 GHz frequency range (X-band, wavelength range 2.4 to 3.7 cm) are transmitted towards the sea surface. Penetration depth of microwaves into the water is only a fraction of the wavelength, and the sea surface reflects the radar pulse

sensor:	SLAR	UV/IR	MWR
model	Ericsson	Daedalus AADS 1221	Ericsson UAZ 10301
frequency/Ghz	9.4		35
or			
wavelength/μm		.32–.38 (UV) 8.5–14 (IR)	
polarization	vertical	unpolarized	horizontal
peak power/KW	10		
pulse rep. rate/kHz	1.0		
pulse width/μs	0.5		
ins. fov/mrad	9 horizontal 650 vertical	5	42
total fov/degrees		87	37
scan rate/Hz		160	2.8–11.2
electric power/VA	420	420	160
total weight/kg	70	29	25

Tab 2 Specifications of remote sensing instruments in the first generation maritime surveillance aircraft DO 28 D2. Data adopted from SSC documents.

perfectly. Wind induced capillary and short gravity waves on the water surface with wave slopes perpendicular to the incident radar pulse give rise to signal returns back to the radar antenna. This effect yields radar images that resemble well to visually observed sun glitter, also caused by the sea surface roughness. However, the physical mechanism which explains quantitatively the backscatter efficiency, is Bragg scattering of the radar pulse on periodic water waves with wavelengths having about the same lengths as the radar wavelength (see, for example, Ulaby et al. 1982).

Waves on the sea surface are sensitively damped by surface films of mineral oil. Therefore, almost no radar echo is obtained from oil-covered areas, and this is the basic mechanism of oil spill detection with radar (Fig 1).

The radar antenna is perpendicularly mounted on the side of the aircraft, looking perpendicular to the flight track. By that way, a map of the backscatter from the sea surface normal to the flight direction of the aircraft is obtained upon the time-resolved registration of the radar pulse return. The detection range depends on the flight height and the sea state, and on instrumental factors as the pulse energy and the polarization, and reaches values of typically 20 km for oil slicks detection.

Ground resolution Δr in the cross-flight direction is a function of the radar pulse width τ according to $\Delta r = \tau c/(2\cos\Theta)$, with c the light velocity and Θ the depression angle of the resolved pixel. A 100 ns pulse length yields a cross-flight resoution of 15 m. With real-aperture radars (RAR), as they are generally utilized for maritime surveillance, the resolution in the along-flight direction depends on the angle of divergence of the radar beam, called antenna beam width, and on the distance to the sea surface.

The antenna beam width is roughly given by λ/L radians, with the radar wavelength λ and the antenna length L. Hence, the ground pixel size obtained with radar from low-flying aircraft is in the order of 100 m^2.

Ground resolution along the flight track can be improved by about a factor of 10, if the synthetic aperture radar (SAR) principle is utilized. Here, the motion of the aircraft allows for the "synthetic" generation of an enlarged antenna size. This technique is generally utilized with radars on satellites because of the large distance to the ground. Application onboard aircraft for regular maritime surveillance has not yet been envisaged because of the still high price of these sensors.

An important characteristic of the SLAR is its ability to detect oil slicks during day and night, and under practically all weather conditions. Waves on the sea surface, that are efficiently damped by oil slicks, are found at wind speeds between 3 to 7 bft.

Limitations arise from the occurrence of other organic substances than oil which produce films on the sea surface: e. g., certain surface-active exudates of plankton are known to produce monomolecular layers with a thickness of about 10^{-3} µm. These layers give rise to about the same damping of waves (Hühnerfuß et al. 1985). Therefore, they cannot be distinguished from oil spills in the radar image and often give occasion to false alarms.

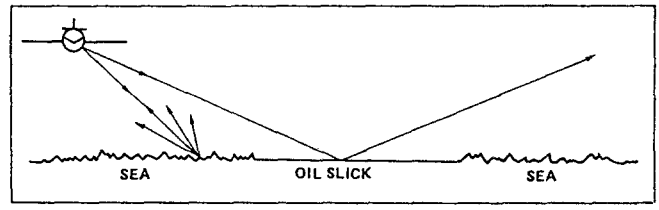

Fig 1 Principle of detection of slicks on the sea surface with radar. The covered area has a width of about 3 to 30 nautical miles normal to the flight direction, depending on the sensor characteristics and the sea surface roughness. (adopted from Gillot and Tosselli 1985)

UV/IR line scanner

The UV/IR scanner is a passive short-range sensor for measuring radiation from the sea surface below the aircraft in the ultraviolet (0.32–0.38 µm) and in the thermal infrared (10–12 µm) portion of the electromagnetic spectrum. A mirror scanning across the aircraft flight direction allows for mapping line by line, yielding images 400 m wide from 1000 ft flight altitude, with a ground resolution of a few metres.

The UV detection channel registers sunlight reflected from the sea surface in this wavelength range. Therefore, the sensor operats during the day and with sunlight only, and clear visibility to the ground is essential. Detection of oil is based on its effect of increasing the reflectivity of the sea surface. This can be observed even with very thin sheens of less than 0.1 µm thickness. The upper limit of the dynamical range is about 10 µm.

However, only a relative information on the film thickness is derived from UV images. In addition to the sunlight illumination, the signal depends on the refractive index and absorbance of the surface film, and on the UV radiance leaving the water column. Algorithms for estimating the film thickness quantitatively have not been investigated, so far. Other substances than oil – e. g., plankton blooms – can produce images which resemble to oil spills. This makes it difficult to detect oil, unambiguously.

The IR channel of the UV/IR scanner measures the brightness temperature of the sea surface in the thermal infrared. Temperature differences between oil and water are induced by the higher absorption of daylight in oil compared with water. This yields a temperature increase over oil spills by a few degrees compared with the surrounding water, depending on illumination, wind, and other factors. The film thickness that shows such temperature differences covers a range of about 100 µm up to a few millimeter. Temperature differences have been observed also in the dark where the oil appears to be colder, an effect which has been attributed to the lower emissivity of oil in the thermal infrared. A discussion of these phenomena is found in Goodman (1989).

Year	1983*+	1984*	1985*	1986	1987	1988	1989
number of flights	58	239	211	197	251	275	262
flight hours	72	307	284	493	530	614	576
observed oil spills	104	186	190	119	138	104	160
identified polluters	11	12	16	13	6	10	10
oil covered suface/km^2	241	244	294	273	50	87	150
discharged oil quantity/m^3	287	696	879	466	103	77	102
oil spills per flight hour	1.4	.6	1.5	.24	.26	.17	.28

* flights performed with the Dutch Maritime Patrol Aircraft
\+ only 6 months

Tab 3 Annual results of aerial surveillance in the German responsibility area of the North Sea and the Baltic. Bustorff, pers. comm.

Because of these ambiguities, a quantitative film thickness scale cannot be obtained from thermal images. However, IR data can be obtained during day and night, and their quality is less sensitive to bad visibility conditions than the UV data.

Experience Obtained with Maritime Surveillance

The two DO 28 D2 surveillance aircraft equipped with these instruments have been operated since the beginning of 1986 with about 250 flights and up to 600 flight hours per year. Areas of investigation are the German responsibility areas of the North Sea and the Baltic Sea, with emphasis on the main shipping routes, and with continuously changing flight patterns. Roughly 100 to 150 pollutions have been observed yearly, see Tab 3. To give an example, Fig 2 shows the geographical distribution of oil spills identified from board aircraft in 1989.

Operational experience obtained so far with the DO 28 surveillance aircraft, and reliability of the sensors utilized

Fig 2 Oil spills observed in 1989 with airborne maritime surveillance in the German responsibility area of the North Sea and the Baltic Sea. The figure was made available by U. H. Bustorff, Federal Special Unit for the Abatement of Oil Pollution, Cuxhaven, Germany.

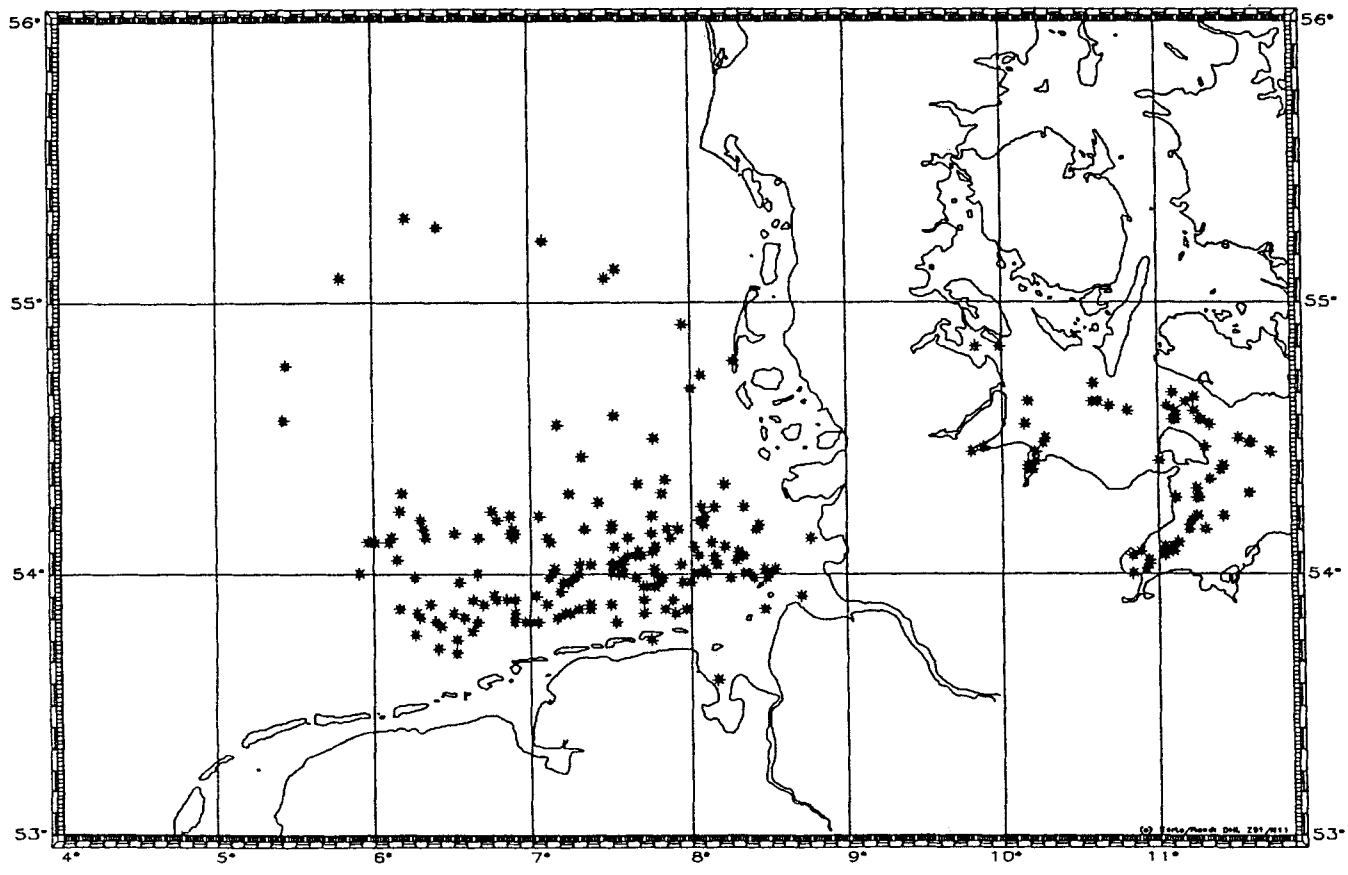

for oil spill detection, have been reported in detail by Schroh and Bustorff (1989). In summary, the use of aircraft for maritime surveillance shows a deterrent effect, if a reduction of controlled oil pollutions is considered to be the essential goal.

Airborne survey in German waters was taken on for the first time in 1983/85 with the Dutch maritime patrol aircraft. An average of up to 1.6 oil spills per flight hour was observed at this time. This high number of oil spills has drastically decreased meanwhile (Tab 2), and this effect is attributed to maritime surveillance.

However, it is stressed by the responsible authorities that, in addition to the detection, localization and mapping of relative film thickness distributions of spills, a more quantitative analysis of pollutants would be an important improvement of aerial surveillance. In particular, this concerns

- an identification of the type of substance within a slick, i. e., the distinction of pollutants and non-toxic substances like, for example, biogenic films

in order to reduce the number of false alarms,

- a classification of the type of pollutant, according to oil classes like heavy, medium, and light crude, or refined products, and the identification of chemical pollutants,

and

- a quantitative measurement of the thickness distribution of spills, and, hence, a reliable evaluation of the pollutants volume,

for improving the quality of evidence of remotely sensed data in case of controlled discharges of small amounts of pollutants. This also concerns improvements of methods necessary for estimating the spill thickness distribution in cases of large quantities following accidents, and a better support of recovery operations based on such data.

Fig 3 Schematic of the 2nd generation Maritime Surveillance Aircraft which will be put into operation in early 1991. The Side-looking and Forward-looking Airborne Radar (SLAR, FLAR)), UV/IR Line Scanner, and the TV cameras are taken over from the 1st generation DO 28 aircraft. Central Operator Console (ZOP) and Data Down Link (DDL) are new components. The newly developed Microwave Radiomemter (MWR) and the Laser Fluorosensor (LFS) will be ready for aircraft integration in late 1992.

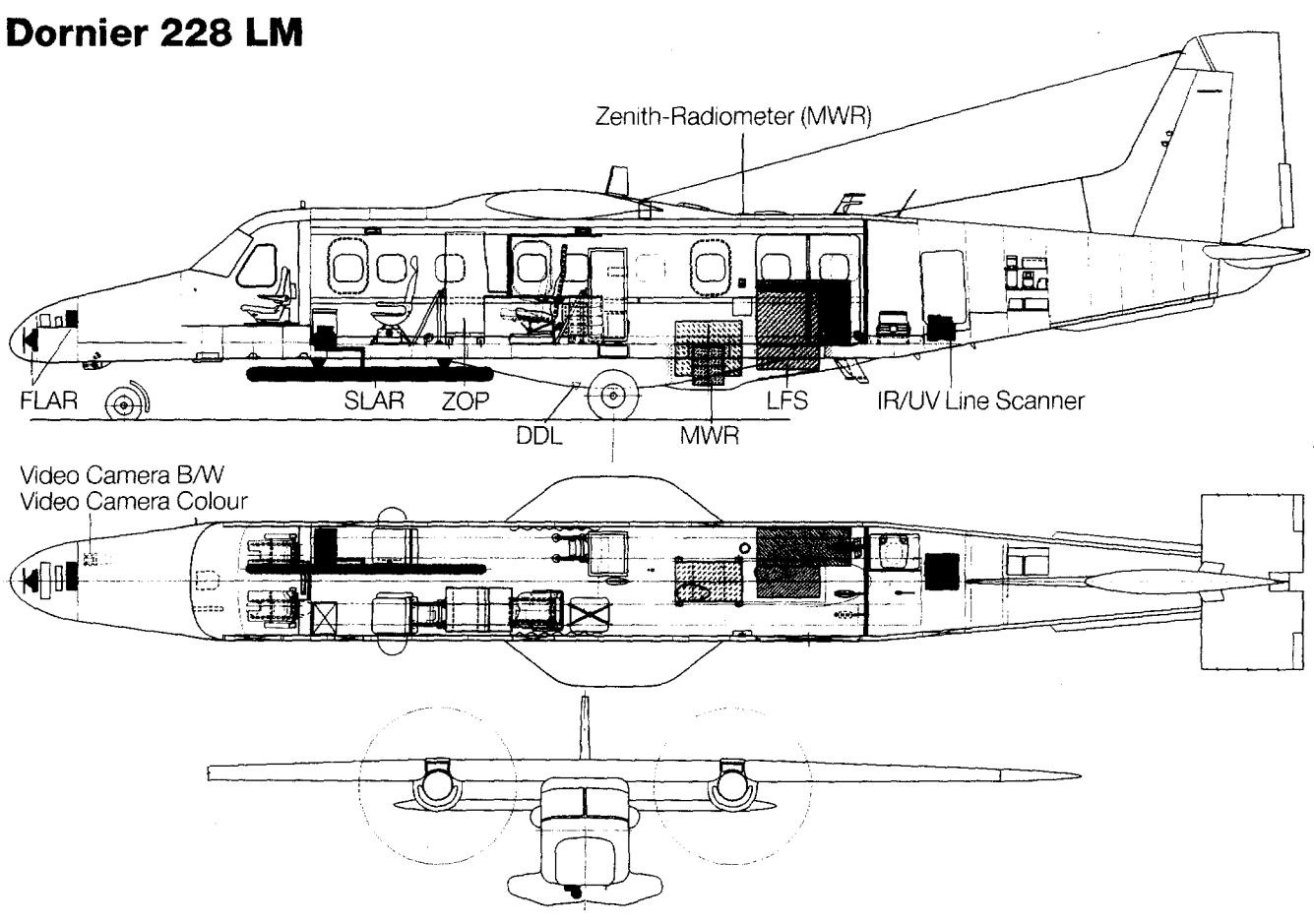

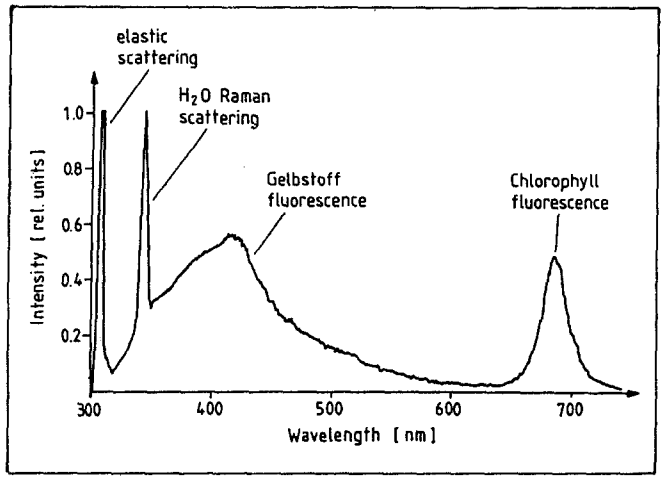

Fig 4 Emission spectrum of a natural water sample taken from the German Bight. Excitation wavelength is 308 nm. The peaks at 308 and 344 nm are due to elastic scattering and water Raman scattering, respectively. The broad fluorescence with a maximum near 420 nm is due to gelbstoff. The fluorescence peak at 685 nm is due to chlorophyll a. (Hengstermann and Reuter 1989)

Finally, an increase of the number of flight operations is desired, as well as a higher endurance of the aircraft. This shall allow for a better coverage of the North Sea, which is also important within the programmes of international cooperation for maritime surveillance.

The time of operation of the two surveillance aircraft which were procured in 1985 was appointed to 5 to 8 years. A perspective for realizing the above-mentioned improvements came in sight from the need of procuring a new aircraft, and from the results of sensor developments at research institutes. Microwave methods had been investigated at the Institute for Radio Frequency Technology, DLR Oberpfaffenhofen, and laser fluorosensing at the Physics Department of the University of Oldenburg, including field tests of experimental sensors in airborne campaigns (see respective publications in Gillot and Toselli 1985; Gillot 1987).

Therefore, the Bundesministerium für Verkehr decided in 1988 to realize a new maritime surveillance system. In addition to approved sensors utilized up to this time in the first generation aircraft, the new system will include newly developed instruments to meet the requirements mentioned.

The new Maritime Surveillance System

A Dornier DO 228-212 aircraft was selected as the carrier with modifications of the avionics (OMEGA and GPS navigation, weather radar, data down link to combating ships), and of the fuselage for allowing an integration of remote sensing instruments.

The basic requirements on the first generation Maritime Surveillance System are applied also to the new system. SLAR, UV/IR scanner and cameras, which had been successfully utilized in the DO 28 aircraft, are integrated into the new DO 228, supplemented with a new Central Operator Console (ZOP), developed by Krupp MaK Maschinenbau, Kiel.

In addition to this, the aircraft is being prepared for the later integration of a laser fluorosensor (LFS) and a microwave radiometer (MWR). These instruments are under development at the University of Oldenburg and at DLR Oberpfaffenhofen, respectively, in cooperation with Krupp MaK, and with support of the Bundesministerium für Forschung und Technologie, Bonn.

The laser fluorosensor and the microwave radiometer allow a deeper analysis of oil spills. This includes a quantification of the spilled volume over a range covering small discharges up to accidental events, and a classification of oil types. The LFS can be applied further in the field of marine biology and oceanography for measurements of plankton distributions and coastal circulation.

Prototype versions of these sensors will be ready in late 1991. Aircraft integration of operational versions, which will be qualified for a continuous application in maritime surveillance, is anticipated for late 1992. Their measuring principles and technological layout are discussed in the next section.

Other improvements of the system, Fig 3, concern the endurance of the aircraft: a flight time of 3 to 4 hours is anticipated during oil combating operations following accidental discharges. More than 1000 flight hours per year will be achieved in surveillance which is almost a factor of two more compared with the DO 28 used formerly.

New Instruments

The Laser Fluorosensor

The LFS is an active sensor for analyzing the upper layers of the sea from aircraft flight heights of 100 to 300 m in the near-nadir range. The instrument consists of a high power pulse laser, and of a telescope receiver and spectrograph for the detection of laser induced fluorescence and scattering. The method can be applied during day and night and is not sensitive to the sea state within the practically interesting range of 0 to 7 bft. However, a sufficiently clear atmosphere between the sensor and the sea surface is mandatory.

The laser wavelength is chosen in the UV or blue/green portion of the spectrum where a penetration depth of a few meters into the water column can be achieved. At these wavelengths, fluorescence of suspended and dissolved organic matter of natural origin can be excited, Fig 4; chlorophyll contained in algae, and gelbstoff, also denoted as humic substance or *d*issolved *o*rganic *m*atter DOM.

In addition to gelbstoff and chlorophyll fluorescence, Raman scattering of water molecules is observed. The turbidity of seawater can be evaluated from this signal

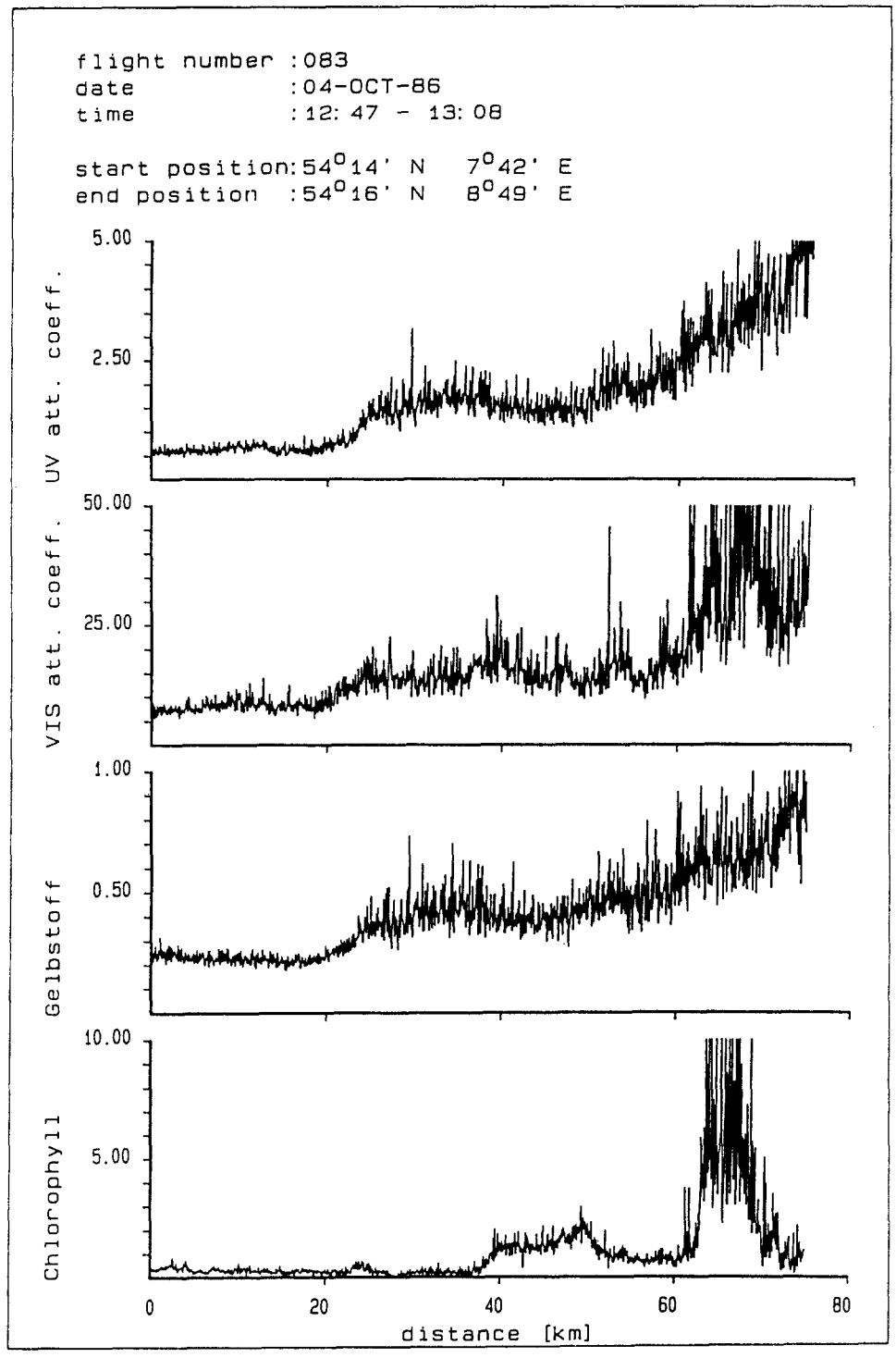

Fig 5
Hydrographic data obtained with an experimental fluorosensor in the German Bighi along a wesi-east flight track as indicated. The curves display nearsurface values of the relative attenuation coefficients at UV and blue-green wavelengths, and of gelbstoff and chlorophyll concentrations. At position 23 km, northwest of Helgoland, a river plume front is found whith separates water with low gelbstoff content from water influenced by river Elbe run-off with increased values of this substance. High chlorophyll concentrations are found near the coastline, indicating the presence of a plankton bloom.

(Bristow et al. 1981). It is also used for correcting the intensities of fluorescence signals with respect to the optical penetration depth into the water column. Therefore, fluorescence intensities which are normalized to water Raman scattering correspond to concentrations of fluorescent substances.

These parameters are relevant for describing biological and physical conditions in coastal waters. Chlorophyll is an indicator for phytoplankton, these measurements allow estimating biological productivity. Gelbstoff is closely related to river water run-off which is the dominant source of this material near the coastline. Gelbstoff is sufficiently stable for time scales which are typical for coastal circulation. Therefore, its measurement yields a description of transport and mixing of river water, and of substances contained herein that have a conservative

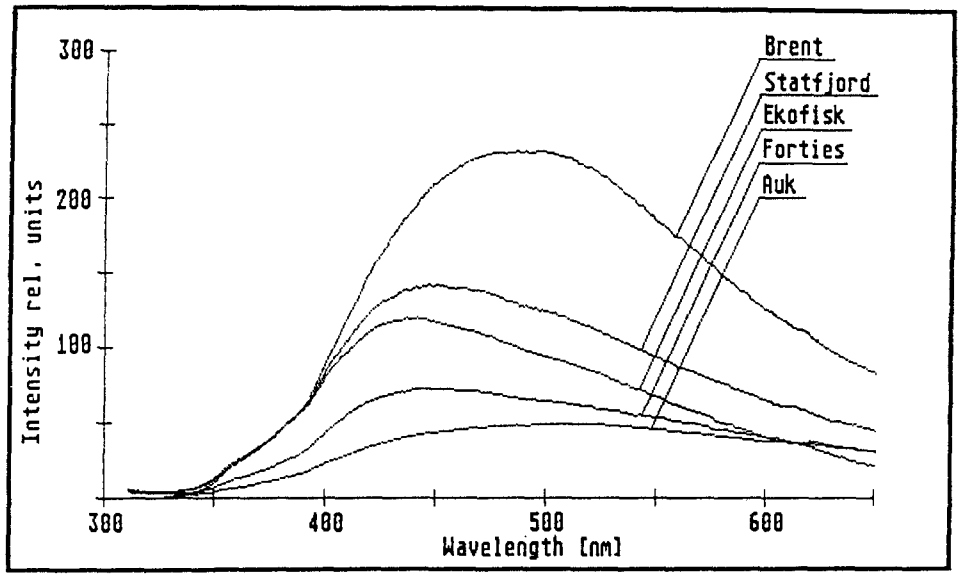

Fig 6
Emission spectra of North Sea crude oils. Same excitation wavelength as in Fig 4.

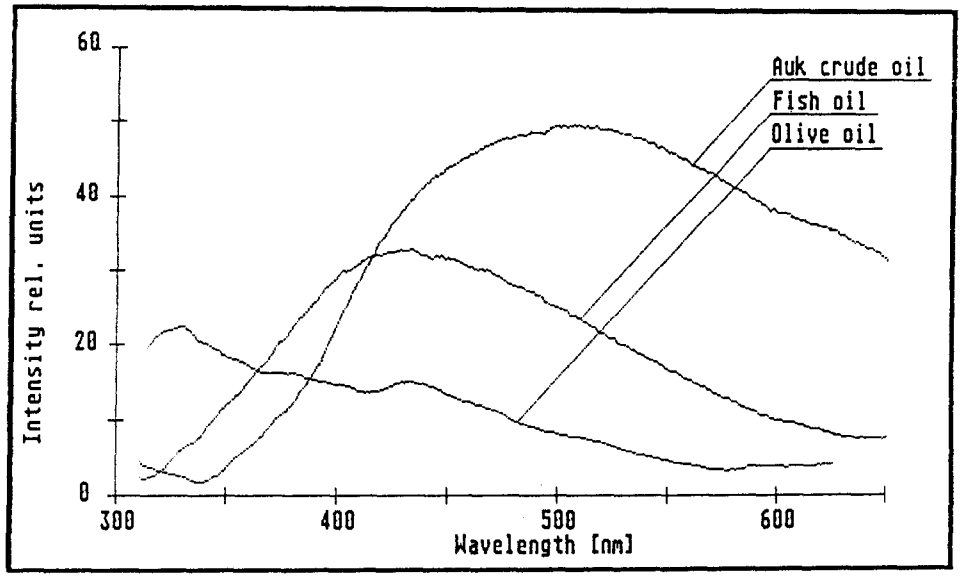

Fig 7
Emission spectra of fish oil and oliv oil. The Auk crude oil spectrum shown in Fig 6 is given for comparison. (Hengstermann and Reuter 1990)

characteristic similar to gelbstoff. An example of such data obtained in the German Bight is shown in Fig 5.

Mineral oil gives rise to fluorescence with an intensity comparable to that of gelbstoff. The spectra cover the entire visible range. Their shape differs from one oil type to another (Fig 6), and this is the basis for an oil type classification with fluorescence spectroscopy. The concentration of fluorescent compounds in animal oil and vegetable oil is much lower (Fig 7), which yields a specifically different fluorescence signal, thus allowing a discrimination of these substances.

In case of small amounts of oil on the sea surface which give rise to thin partially transparent films, a superimposition of gelbstoff and oil fluorescence is observed (Fig 9 a). Their balance allows a sensitive estimation of changes of the optical characteristic of the oil due to weathering or separation into different physical fractions (Hengstermann and Reuter 1990).

The thickness of oil films can be derived from the water Raman scatter intensity measured above the slick and above the oil-free surrounding water (Hoge and Swift 1980). The ratio of these intensities is a function of the absorption coefficient a of light within the oil film and of its thickness d according to $exp(-ad)$. A solution for the film thickness requires an estimate of the absorption coefficient which must be derived from optical data catalogs.

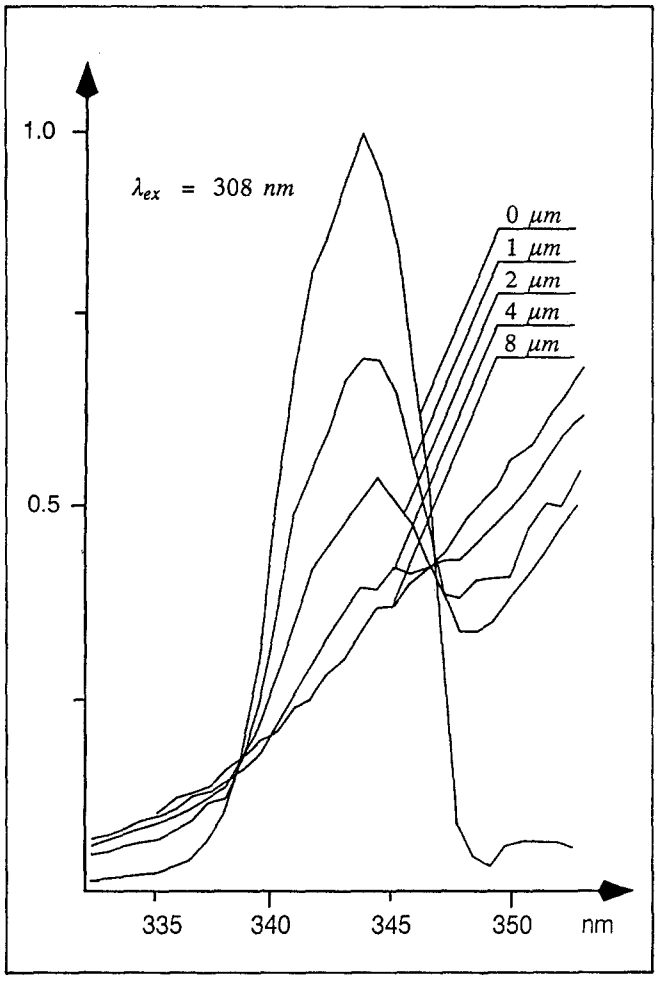

Fig 8 Fluorescence spectra of Statfjord crude oil films on the water surface, near the wavelength of water Raman scattering. The curves were obtained with a setup that simulates a laser fluorosensor measurement. The water is free of gelbstoff compounds, hence the Raman scatter peak is observed without gelbstoff background (see Fig 4 for comparison). With increasing oil film thickness its intensity is depressed due to absorption of light within the oil. At 8 µm film thickness the Raman peak disappears, and only oil fluorescence is observed (Diebel-Langohr et al. 1985)

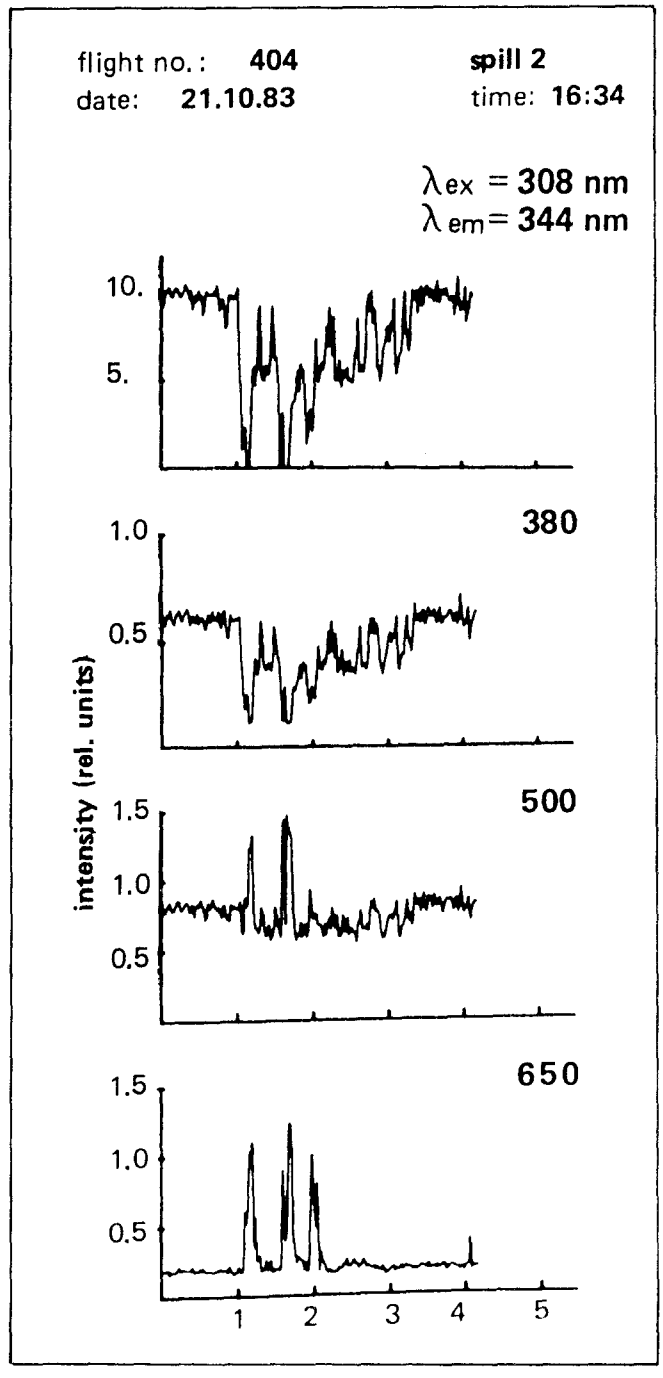

Fig 9 a Laser fluorosensor measurement of a heay fuel-oil spill. Laser wavelength is 808 nm. Signal intensities at the water Raman scatter wavelength 344 nm, and at the fluorescence wavelengths 880, 500 and 650 nm are shown. The oil spill extends from km 10 to 8.5. Outside this area gelbstoff fluorescence is observed. (Diebel-Langohr et al. 1985)

The absorption coefficient of oil takes on values of about 1 μm^{-1} typically in the near UV which makes the method very sensitive for film thickness measurements in the range of a few micrometre (Fig 8, 9 b). Discharges of more than 60 litres of oil per nautical mile which represent violations of the MARPOL convention, give rise to films in this thickness range.

Based on the experience obtained with experimental sensors, a new laser fluorosensor especially designed for the analysis of marine pollution is now developed. The instrument, shown in Fig 10 and 11, meets the qualification standards for aircraft application. A first integration into a DO 228 research aircraft of DLR Oberpfaffenhofen and flight tests were done in October 1990. Extensive campaigns are planned in the North Sea in the first half of 1991.

Particular emphasis is put on the capability of two-dimensional mapping of the sea surface which allows for an

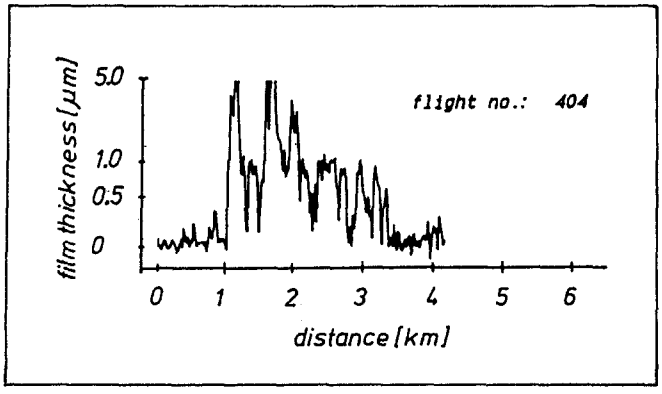

Fig 9b Thickness of the oil film calculated from the intensity of water Raman scattering

optical probing of small geometric scales. An example of the pixel distribution utilized for oil spill mapping is given in Fig 12. In each pixel the spectrum of fluorescence and water Raman scatter is obtained at 12 detection wavelenghts (Tab 4). From these data,

- information on substance types on the sea surface are derived (toxic/harmless/natural), and pollutants are classified (e.g. heavy/medium/light fuel oil)
- the film thickness of oil spills is calculated in the range of about 0.1 to 10 µm,
- swimming chemicals and substances drifting underneath the sea surface are detected, within the penetration depth of the method.

In addition to these measurements, other applications in the field of oceanographic remote sensing are foreseen, as well. The UV excimer laser wavelength enables sensitive measurements of gelbstoff from which a mapping of hydrographic conditions in coastal waters is obtained. The wavelength chosen for the dye laser provides a good fluorescence efficiency of chlorophyll. Hence, the dynamics of plankton growth can be observed on the basis of regularly performed flights.

The Microwave Radiometer

In contrast to the SLAR, the MWR is a passive near-range sensor which measures the natural (thermal)

Fig 10 Schematic of the laser fluorosensor (LFS). Position of the scanner is above a bottom hatch of the aircraft which is sealed by a quartz window for protection of the optioal components. The detector unit contains the 12 channel spectrograph and gated integrator, and the computers for sensor control and substance classification.

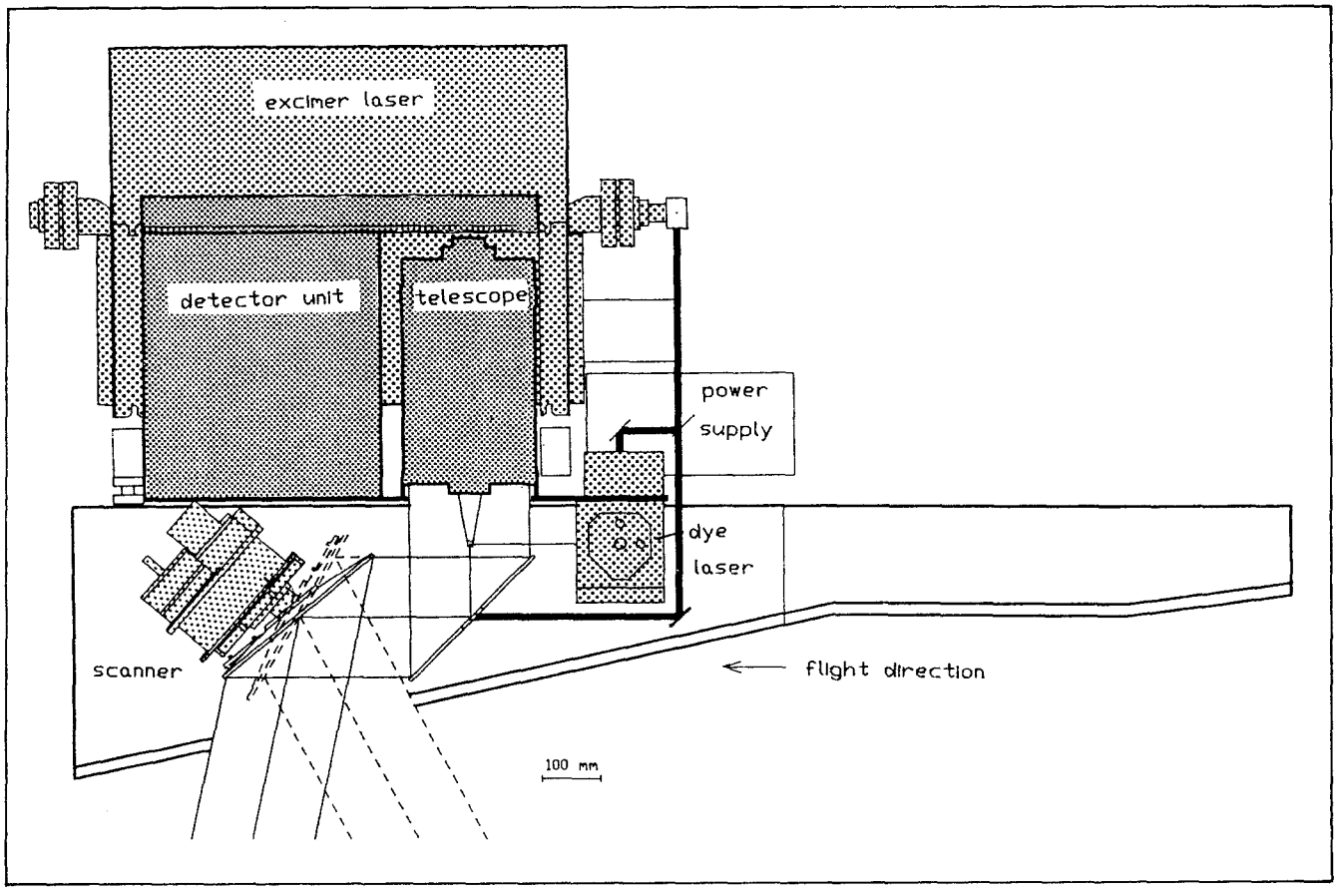

Tab 4
Laser Fluorosensor characteristics (preliminary status Nov. 1990)

Operating properties		
size (l x w x h)	1270 x 355 x 978 mm excimer laser 961 x 460 x 944 mm detector unit	
weight	300 kg	
flight height	1000 ft. typ.	by daylight
	3000 ft. typ.	by night
aircraft ground speed	100–200 knots	
electrical power	1.0 kVA	in standby
	3.4 kVA	at 110 Hz pulse rate
data interpretation	real time	
distance of eye-safe operation	>50 m	
Lasers:	XeCl excimer	dye
emission wavelength	308 nm	382 nm
pulse energy	150 mJ	20 mJ
pulse length	20 ns	15 ns
beam divergence	5 mrad	3 mrad
repetition rate	200 Hz max 110 Hz av.	20 Hz
Receiver telescope:	reflective, Schmidt-Cassegrain	
entrance aperture	20 cm	
f-number	f/10	
Scanner:	conical type	
full scan angle	28° across-flight, 35° in-flight	
scan frequency	≦20 Hz, selectable	
swath width	150 m 1000 ft. flight height	
pixel-to-pixel distance	10 m typ. 1000 flight height, 200 Hz max. laser rep. rate	
Spectrograph:	12 discrete channels, modular	
wavelengths/nm	344	Raman scatter $\lambda_{las} = 308$ nm
	330/365/380	Raman baseline, oil and gelbstoff fluorescence
	440 nm	Raman scatter $\lambda_{las} = 382$ nm
	410/470 nm	Raman baseline, oil and gelbstoff fluorescence
	500/550/600/650	oil and gelbstoff fluorescence
	685	chlorophyll fluorescence
wavelength selection	dichroic splitters, interference and blocking filters	
optical bandwidth	10 nm typ.	
detectors	head-on PMT, range gated	
A/D conversion	12 channel gated integrator, 11 bit	
Computers:	all VME-Bus, 68020 processor, 16 MHz	
sensor control	selection of lasers and detectors, control of measuring cycle, film thickness estimation	
classification	identification of substances	
image processing	component of central operator console: images of LFS ground pixel distribution, evaluation of multisensor imagery, data storage on streamer or optical disk	

multispectral electromagnetic radiation of matter in the centimetre and millimetre region from typical flight altitudes of 300 to 1000 m. As a passive instrument the MWR consists of antenna and receiver elements, only. As a microwave sensor it also profits from an extensive all-weather capability.

From the present point of view, the quantitative determination of thickness and volume of oil layers floating on the sea surface is the main task of the MWR. In doing so, it utilizes interference phenomena induced by the upper and lower boundaries of the oil layer comparable to the colour phenomena in the optical region for thin layers. This phenomenon, in fact, is sensitive to the ratio of the layer thickness and the wavelength. Thus the microwave radiometer realizes a method for unambiguous measurement of thickness in a range of 50 micrometre to several millimetres.

Basic requirements for a MWR of second generation are the registration of oil layers also in the thickness range below 200 μm, a better localization of voluminous parts for reason of improved recovery operations and a better estimation of the oil volume itself (error <50%).

The participation in a series of airborne trials on occasion of the international EC campaign Archimedes in

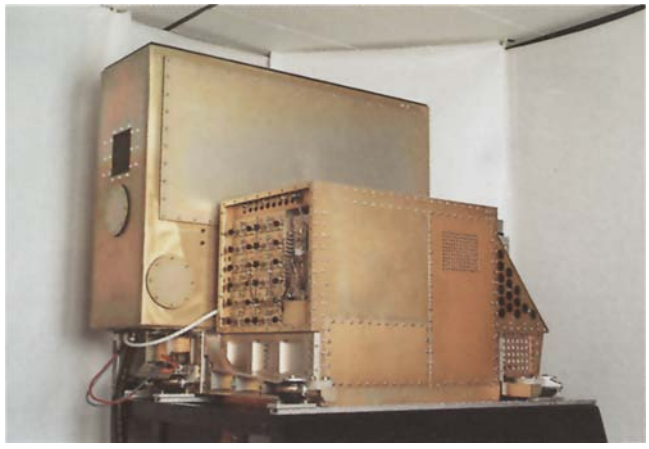

Fig 11 Prototype version of the LFS in the flight test phase, Oct. 1990. In the foreground: detector unit with telescope, scanner and spectrograph. In the background: excimer laser.

the North Sea (Gillot and Toselli 1985; Gillot, 1987; Bekkering, 1990) laid the foundations for the development of a new system. By these measurements, it was possible to study the sensitivity of a multitude of microwave radiometers (wavelength region 6 cm [5 GHz] down to .33 cm [90 GHz]) with respect to different types of oil and water/oil mixtures and for a variety of environmental conditions. For the first time, a 90 GHz radiometer was operated (DLR), which combines the capabilities for high geometrical resolution and registration of layers below 200 µm thickness.

The most essential results are (see also Bekkering 1990):

- estimations of thickness and volume of oil on the water surface works well (error <50%, regularly an underestimation)
- mixtures of oil and water are problematic when water/oil fractions are unknown. Mixtures tend to sink
- 90 GHz images are comparable in quality to IR images. Presently, the microwave radiometer has smaller swath width (Fig 13).
- the optimum package is near 17, 35 and 90 GHz.
- thin oil films could also be sensed qualitatively due to a reduction of the sea surface roughness (Fig 14)
- during hard sea conditions areas with foam could be detected giving rise to an ambiguity problem or false alarm, respectively (Fig 15)
- presently, there is no potential for type identification.

Some of these statements still have to be commented to clarify the scientific background.

Simultaneous measurements at different frequencies are absolutely necessary to avoid ambiguity problems. Theoretically, the measured brightness temperatures oscillate as a function of thickness and frequency (Fig 16). Different thicknesses can generate the same brightness temperature. Because of a rapid variation of thickness along the layer, those strong oscillations never could be registered under realistic environmental conditions, however. The definite selection of the frequencies has to

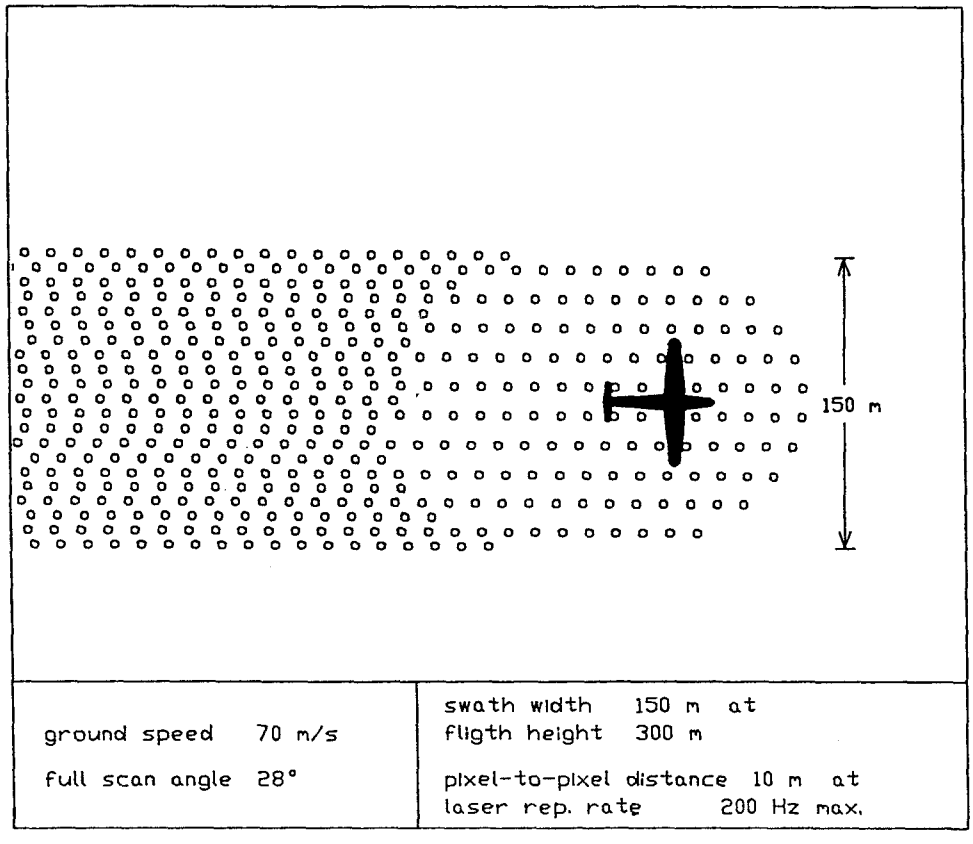

Fig 12
LFS pixel distribution on the sea surface. Laser pulse triggering is controlled by the angle encoder of the scanner, to obtain a mostly uniform pixel coverage. The example shown here will be utilized for oil spill mapping. The parallel operation of excimer and dye laser for hydrographic applications leads to modified ground pixel distributions.

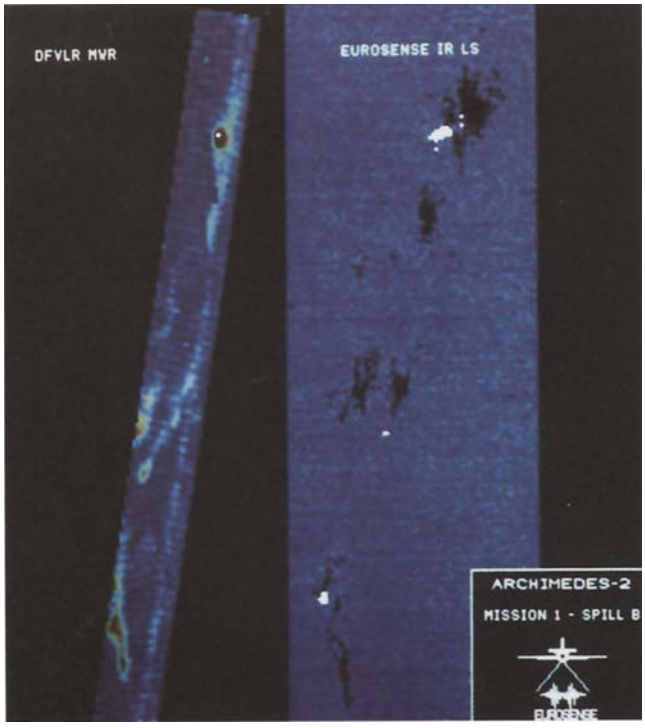

Fig 13 Thin oil measured taken at 90 GHz and in the IR region. Seawater/oil emulsion about 1 hour (90 GHz) and 1/2 hour (IR) after spillage. Scan width 54/200 m. Experiment Archimedes 2, Oct. 1985. IR image: Eurosense-Belfotop.

be done under the aspect of possible interferences due to man-made noise. Measurements at 17 GHz regularly resulted in the best volume estimations for thicker layers. A frequency around 85 GHz is the best compromise with respect to geometrical resolution and bad weather capability. The sensing of thin films which was demonstrated often by aid of 90 GHz measurements could be problematic in the presence of clouds. A simultaneous registration of the sky radiation at this frequency is recommended, therefore, to avoid a misinterpretation because of reflected images of clouds which can give the same signatures as thin films.

The specifications of the new radiometer consider all these experiences. Further, in consideration of the operational use, selfcalibration and low requirements for maintenance were essential design goals.

The radiometer, now under development in a very compact structure, realizes the two-dimensional imaging of oil layers on the sea surface at a swath width of 476 m (altitude 1000 ft), simultaneously at 18.6, 36.5, and 89 GHz. These frequency bands are reserved for passive measurements. Mapping of the sea surface happens by aid of two parabolic mirrors installed in a rotating cylinder. At both ends of the cylinder two identical groups of receivers for the given frequencies are situated which in each case prominently look to one reflector attached via a second plane reflector (Fig 17). During one rotation a complete

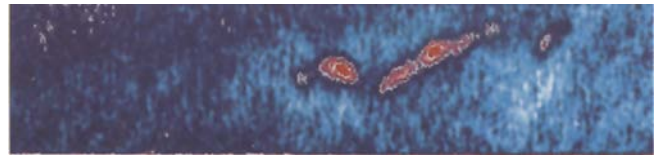

Fig 14 90 GHz image of a crude oil spill taken from an altitude of 1370 m. Resolution is 0.5 K per unit of colour scale, maximum thickness is 0.14 mm (red colour). Volume estimation is 3.41 m^3, which corresponds to 68% of the spilled quantity. The decrease of the brightness temperature in the neighborhood of the thicker parts of the oil spill (white and white/blue colour) is due to a reduction of the sea roughness.

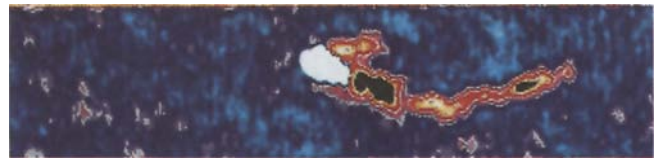

Fig 15 90 GHz image of a vessel during the spillage of heavy fuel oil. Flight height 152 m, scan width 81 m. The image demonstrates ambiguity problems due to the radiation from the stern, the breakwater at the bow and from the foam on the top of the water waves (sea state 5-6).

calibration by measuring the radiation of a cold and a hot load can be carried out. A further 89 GHz radiometer with a fixed antenna directed to the sky measures the radiation of the atmosphere for a region +/−4° (in-flight direction) to +/− 40° around the zenith. The whole system is completely computer controlled. A further computer, which is integrated into the central operator console, directly evaluates the received signals with respect to layer thickness and volume. The frequency channels have

Fig 16 Theoretical values of the microwave brightness temperature for a homogeneous oil layer as a function of thickness and frequency. Nadir angle 0°, clear weather conditions.

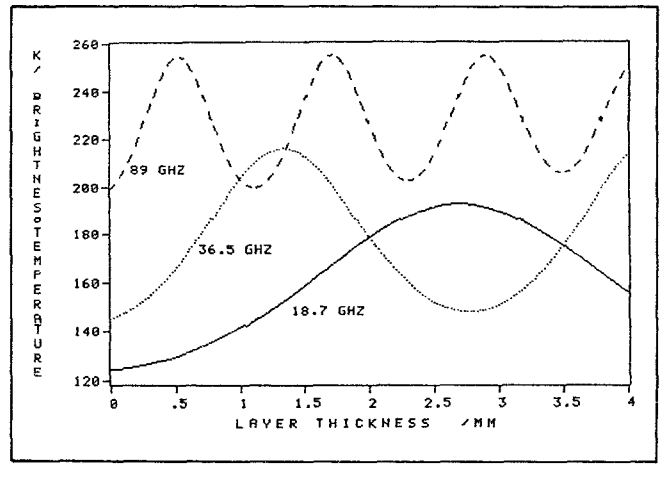

Sensor:	line scanner	sky radiometer
Antenna		
type	rotating offset parabolic reflector, plane reflector 3 scalar horns	sector horn
angular resulution	1: 0.8°	8° * 80°
(3 dB beamwidth)	2: 2.0°	
	3: 4.0°	
scan motion	continous rotation	./.
aspect angle	+/–36°	+/–4° * +/–40°
	off-nadir	off-zenith
scan axis	parallel to longitudinal axis of the airplane	./.
scan frequency	10 revolutions/sec	./.
	20 lines/sec	
Receiver front-end		
frequency band/GHz	1: 86–88 , 90 –92 (DSB)	88. –88.9 and
	2: 36–36.4, 36.6–37 (DSB)	89.1–90 (DSB)
radiometer type	Total Power Radiometer	
receiver type	HETERODYNE	
	(without preamplification exept channel 3)	
intermediate	1: 1–3	0.1–1
frequency band/GHz	2: 0.1–0.5	
	3: 0.6–0.8	
noise temp./Kelvin	1: 530	590
	2: 495	
	3: 495	
Receiver back-end		
type	amplifier with automatic gain control, low pass and analog-to-digital converter	
data rate (each channel)	20.5 kByte/sec max.	20 kByte/sec
signal resolution	12 bit	12 bit
Calibration		
method	hot/cold	
equipment	rotating main reflector looks at definite time sequences to hot or cold load	receiver is switched to hot or cold load

Tab 5 Microwave Radiometer characteristics (preliminary status Nov. 1990)

different geometrical resolutions for the benefit of an optimum utilization for the antenna apertures, especially at 90 GHz. An identical resolution, which is important for an unambiguous estimation of the volume, can be realized numerically, however. A list of the most important specifications of the new MWR is given in Tab 5.

Together with the sensor development a refined theoretical model for data interpretation is acquired. It will take into consideration the sea state and the influence of the atmosphere.

First test flights with the new sensor are foreseen at the end of July 1991.

Central Operator Console

The Central Operator Console (ZOP), developed by Krupp MaK Maschinenbau, Kiel, allows the control of the remote sensing and avionics equipment by a single operator. It acts as the interface to the aircaft, thus transforming the individual sensors to an integrated surveillance system.

The console has been developed especially for aircraft use, with high demands on mechanical construction, size, weight, and power consumption. The components have been chosen with particular emphasis on modularity. Therefore, the Central Operator Console can be adapted easily to other sensors available in the future, and to different types of aircraft.

A VME-Bus computer processes the data in real time. Raw data of the individual sensors are evaluated by use of appropriate algorithms, and displayed on two colour LCD monitors (resolution 200 x 640 pixel) for the readout of individual sensors, or as an imagery combining the results of different sensors on a single screen. In addition to status information of these sensors, the long-ranging SLAR data are shown on a monochrome LCD monitor (512 x 440 pixel resolution). Alternatively, a CRT display can be integrated into the console. Screen-dumps of these images are made for immediate hardcopy, and they can be transmitted via data downlink to ships and land stations.

Sensor raw data, navigational data, and other auxiliary information are stored on streamer tape or optical disk, allowing for a more detailed post-flight data interpretation on the ground.

Acknowledgements

We wish to express our thanks to the industrial partners in the realization of the Maritime Surveillance System, X. Hartl and Dr. G. Deike (Dornier Deutsche Aerospace), J. C. Jensen and Dr. A. Eßlinger (Krupp MaK Maschinenbau), and Dr. Hoffmann (Wissenschaftlich-technische Beratungen), and their colleagues.

We are particularly grateful to the members of the working groups at research institutes, involved in the development of remote sensing instruments, T. Hengstermann, K.-D. Loquay, H. Wang, and R. Willkomm at the University of Oldenburg, G. Kalisch, H. Schreiber, and P. Sliwinski at the German Aerospace Research Establishment.

Development of the Laser Fluorosensor and the Microwave Radiometer is financed by grants from the Bundesministerium für Technologie. We thank Dr. H. J. Kraege and Dr. W. Schött (BMFT), and O. Krause from DLR Projektträgerschaft Umweltschutztechnik, for their continued support and encouragement.

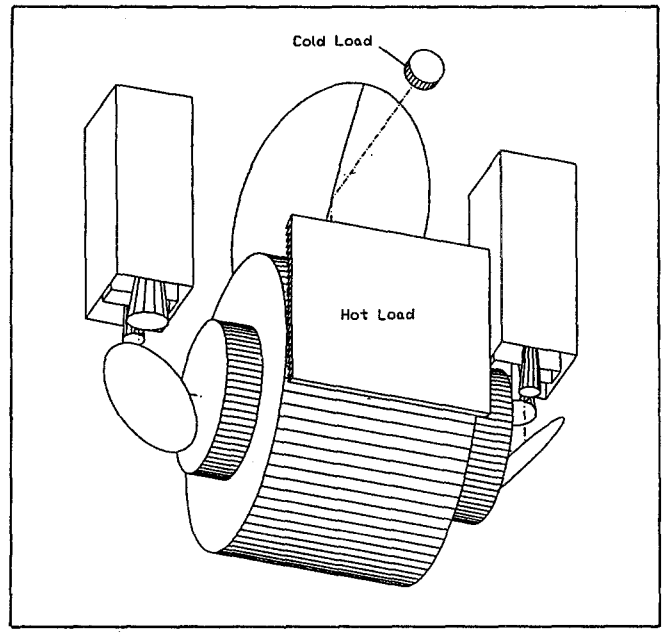

Fig 17 Configuration of the MWR under development. Two parabolic reflectors in a rotating cylinder and two receiver groups realize two scan lines per revolution. Thermal "hot/cold" sources are used for a continuous calibration.

References

Bekkering, J. A.: The Archimedes 2A Experiment. Commission of the European Communities, Series: Environment and Quality of Life. EUR 12674 EN, 83 pp. Luxembourg 1990.

Bergmeijer, P.: Regulations for control and reduction of marine pollution. In: Reuter, R.; Gillot, R. H. (eds.), Remote Sensing of Pollution of the Sea, pp. 34-53. Commission of the European Communities, Joint Research Centre - Ispra Establishment, and BIS University of Oldenburg, S.P.I. 87.46, 1978.

Bristow, M.; Nielsen, D.; Bundy, D.; Furtek, R.: Use of water Raman emission to correct airborne laser fluorosensor data for effects of water optical attenuation. Appl. Opt. 20, 2889-2905 (1981)

Diebel-Langohr, D.; Hengstermann, T.; Reuter, R.; Checchi, G.; Pantani, L.: Measuring joil at sea by means of an airborne laser fluorosensor. In: Gillot, R. H.; Toselli, F. (eds.), The Archimedes 1 Experiment, pp. 123-142. Commission of the European Communities, Series: Environment and Quality of Life. EUR 10216 EN, 228 pp. Luxembourg 1985.

Gillot, R. H.; Toselli, F. (eds.): The Archimedes 1 Experiment. Commission of the European Communities, Series: Environment and Quality of Life. EUR 10216 EN, 228 pp. Luxembourg 1985.

Gillot, R. H.: The Archimedes 2 Experiment. Commission of the European Communities, Series: Environment and Quality of Life. EUR 11249 EN, 238 pp. Luxembourg 1987.

Goodman, R. H.: Application of the technology in North America. In: Lodge, A. E. (ed.), The Remote Sensing of Oil Slicks, pp. 39-65, John Wiley & Sons, Chichester 1989.

Hengstermann, T.; Reuter, R.: Lidar fluorosensing of mineral oil spills on the sea surface. Appl. Opt. 29, 3218-3227 (1990)

Hoge, F. E.; Swift, R. N.: Oil film thickness measurement using airborne laser-induced water Raman backscatter. Appl. Opt. 19, 3269-3281 (1980)

Hühnerfuß, H.; Alpers, W.; Richter, K.: On the discrimination between crude oil spills and monomolecular sea slicks by airborne radar and infrared radiometer - possibilities and limitations. Int. J. Remote Sensing 7, 1001-1013 (1985)

Lodge, A. E. (ed.): The Remote Sensing of Oil Slicks. 165 pp. John Wiley & Sons, Chichester 1989.

Schriel, R. C.: Monitoring of operational discharges from oil production platforms. In: Lodge, A. E. (ed.), The Remote Sensing of Oil Slicks, pp. 77-86, John Wiley & Sons, Chichester 1989.

Schroh, K.; Bustorff, U. H.: Operational discharges in the Federal Republic of Germany. In: The Remote Sensing of Oil Slicks, pp. 87-103, John Wiley & Sons, Chichester 1989.

Ulaby, F. T.; Moore, R. K. Fung, K. A.: Microwave Remote Sensing. Vol. II, 912 pp. Addison-Wesley, Reading, MA 1982.